

The formation of multipoles during high-temperature creep of austenitic stainless steels

P. R. HOWELL

Department of Metallurgy and Materials Science, University of Cambridge, Cambridge, UK

J. O. NILSSON

Sandvik AB, 81101 Sandviken, Sweden

A. HORSEWELL

Laboratory of Applied Physics, Technical University of Denmark, Lyngby, Denmark and Risø National Laboratory, Roskilde, Denmark

G. L. DUNLOP

Department of Physics, Chalmers University of Technology, 412 96 Göteborg, Sweden

It is shown that multipole dislocation configurations can arise during power-law creep of certain austenitic stainless steels. These multipoles have been analysed in some detail for two particular steels (Alloy 800 and a modified AISI 316L) and it is suggested that they arise either during instantaneous loading or during the primary creep stage. Trace analysis has shown that the multipoles are confined to $\{111\}$ planes during primary creep but are not necessarily confined to these planes during steady-state creep unless they are pinned by interstitials.

1. Introduction

The development of dislocation distributions during power-law or dislocation creep has been the subject of a number of investigations (for a recent review see Gittus [1]). A variety of dislocation configurations have been observed and analysed. These include subgrain boundaries [2, 3], dipoles and three-dimensional networks [4]. In this paper it is shown that, in addition to the above, dislocations can be arranged in multipoles which consist of a series of dipoles held together by the interaction between dislocation strain fields of opposite sign. Fig. 1 is a schematic drawing of a multipole dislocation configuration and illustrates the fact that alternate dislocations possess Burgers vectors which are of equal magnitude but opposite in sign.

The observations detailed in this article relate to Alloy 800* (a 20 wt% Cr–30 wt% Ni, Ti-

stabilized, austenitic steel) and a modified AISI 316L steel† (an 18 wt% Cr–12 wt% Ni steel containing small additions of V and N). The compositions of these alloys are given in Table I. The general creep behaviour of these alloys has been detailed elsewhere [5, 6].

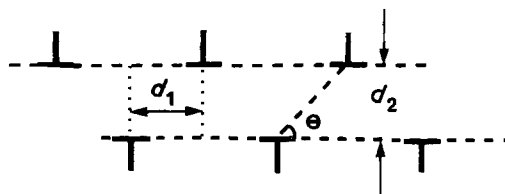


Figure 1 A schematic drawing of a multipole dislocation configuration. In the easy glide stage of low-temperature deformation of single crystals, the dislocations in the multipole lie on $\{111\}$ planes.

*Supplied by Sandvik AB – SANICRO 31.

†Supplied by Uddeholm AB – UHB SS 724 LN.

TABLE I Compositions of the experimental alloys

Alloy	Cr (wt%)	Ni (wt%)	Ti (wt%)	V (wt%)	Si (wt%)	Mn (wt%)	Mo (wt%)	Al (wt%)	C (wt%)	N (wt%)
Alloy 800	21.4	33.2	0.5	—	0.5	0.6	—	0.3	0.014	—
AISI 316 L	18	12	—	0.4	0.5	1.7	2.7	—	<0.03	0.1

2. Experimental procedure

Prior to creep testing, specimens of Alloy 800 were solution-treated at 1000°C, aged for 100 h at 850°C and then furnace cooled. This heat treatment led to a fairly coarse intergranular dispersion of TiC precipitates. The average grain size was 25 μm . The AISI 316L specimens were solution-treated at 1100°C and water quenched. This treatment resulted in a supersaturated single-phase microstructure with an average grain size of 60 μm .

Constant-load creep tests were conducted on smooth bar specimens in air at 800°C (Alloy 800) and at 650°C (AISI 316L). Thin foil specimens for transmission electron microscopy were taken

from interrupted creep tests in which the specimen had been cooled under load.

3. Results

3.1. General intergranular defect structures

As reported earlier [5], creep of Alloy 800 at 800°C at applied stresses, σ , of $\sigma \lesssim 5$ MPa occurs almost entirely by diffusion creep and virtually no matrix dislocation activity is observed. At higher stresses ($\sigma > 5$ MPa) dislocation creep becomes more significant and increasing dislocation activity is observed. Typical examples of defect structures generated during creep at $\sigma = 30$ MPa are shown in Fig. 2. During the early stage of

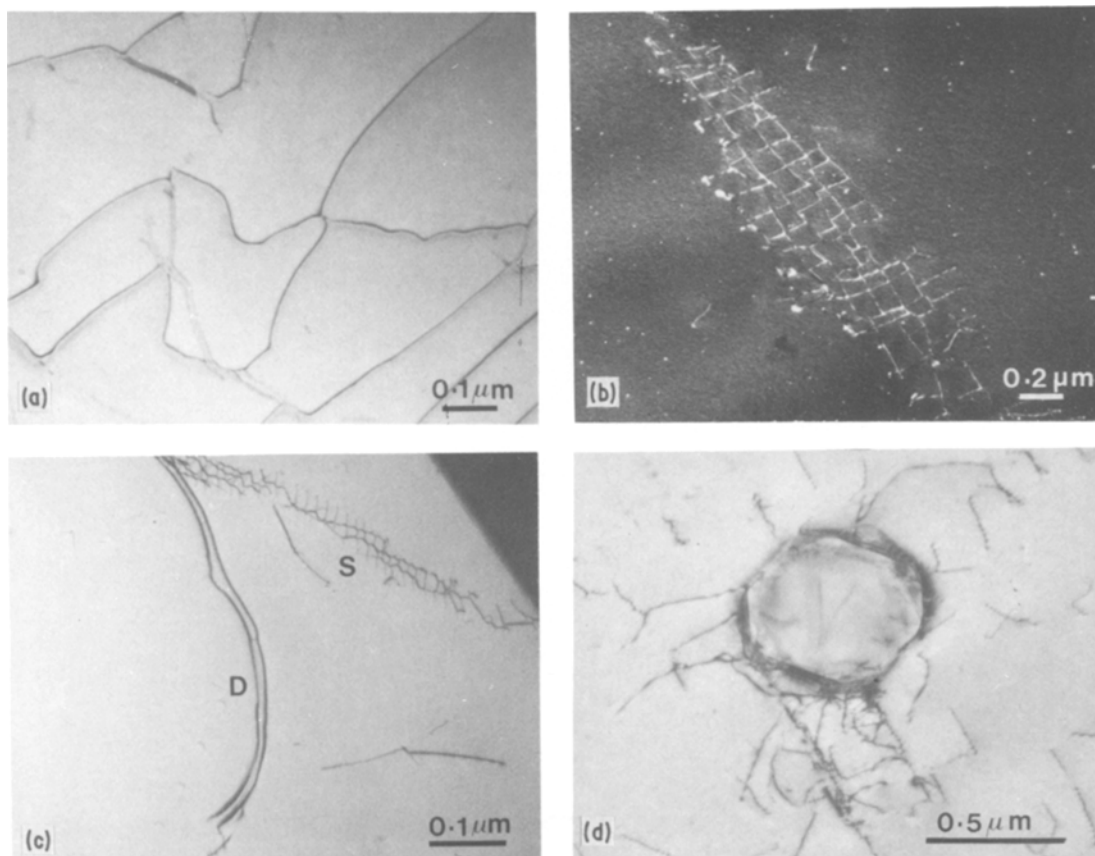


Figure 2 Dislocation distributions observed in Alloy 800 crept at a stress of 30 MPa. (a) An irregular dislocation network observed during primary creep (strain, $\epsilon = 1\%$); (b) weak-beam image of a sub-grain boundary formed during secondary creep ($\epsilon = 5\%$); (c) a dipole (D) and an ill-formed sub-grain boundary (S) in the region of a high-angle grain boundary ($\epsilon = 5\%$); (d) dislocation tangles in the vicinity of a large intergranular TiC precipitate ($\epsilon = 5\%$).

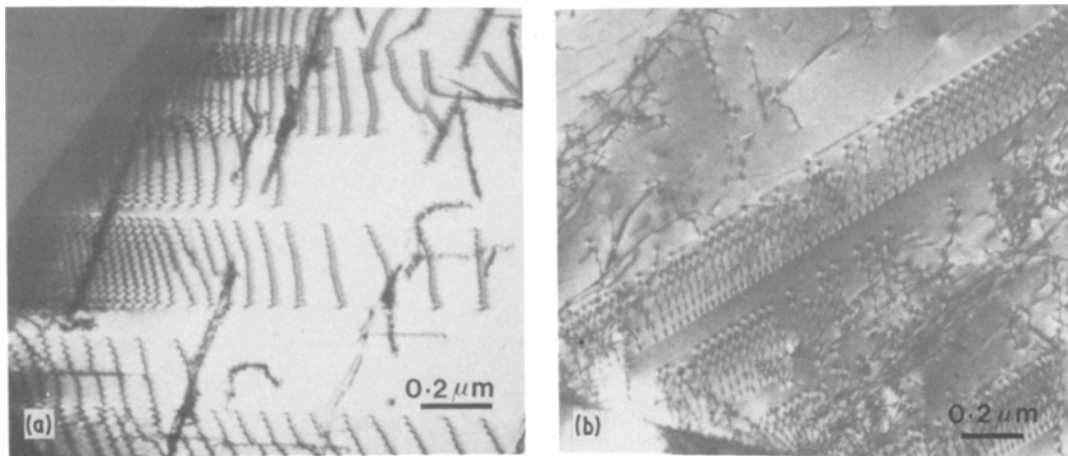


Figure 3 Examples of dislocation pile-ups in AISI 316L after creep at 150 MPa ($\epsilon = 1\%$). (a) A series of closely-spaced pile-ups in the vicinity of a grain boundary; (b) pile-ups within the body of a deformed grain.

primary creep, loose two-dimensional dislocation networks form (see Fig. 2a) and these become well developed sub-grain boundaries during steady-state creep (see Fig. 2b). Dipoles are observed during both primary and secondary creep (see Fig. 2c) and the few large intergranular TiC particles were invariably associated with enhanced dislocation activity* (see Fig. 2d).

The dislocation structures produced during creep of AISI 316L are markedly different to those found in Alloy 800. In AISI 316L creep deformation at 650°C is virtually undetectable for $\sigma \leq 130$ MPa and little dislocation activity is observed [6]. At higher stresses the deformed microstructure is dominated by dislocation pile-ups

which develop during the first few seconds of creep testing [6]. These pile-ups are preserved throughout steady-state creep due to the pinning action of copious fine VN precipitation. Typical examples of pile-ups after creep at $\sigma = 150$ MPa are shown in Fig. 3.

3.2. Observation of multipoles in Alloy 800

In addition to the defect structures illustrated in Fig. 2, multipole dislocation configurations were frequently observed. Multipoles were found in material which had experienced primary or secondary creep (Fig. 4).

Adjacent dislocations in individual multipoles were identified as having Burgers vectors of op-

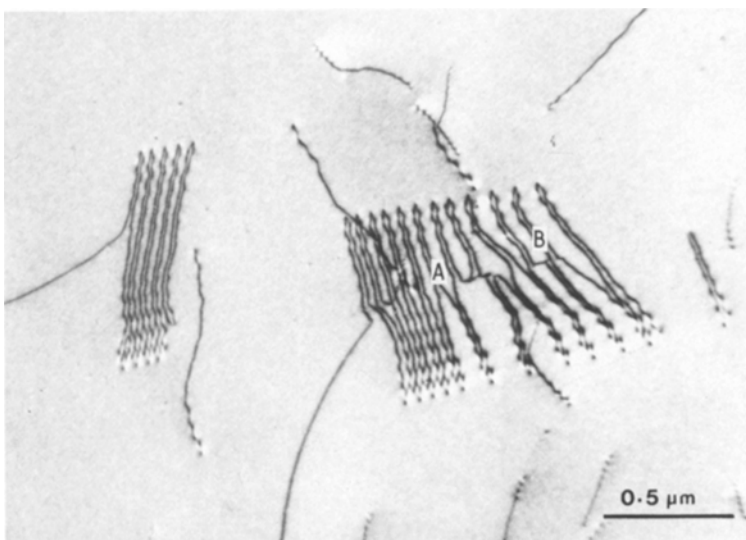


Figure 4 Two multipoles in Alloy 800 deformed in secondary creep. Note that individual locations can change dipole partners for example, at A and B).

*These large TiC precipitates were not dissolved during the solution treatment at 1000°C.

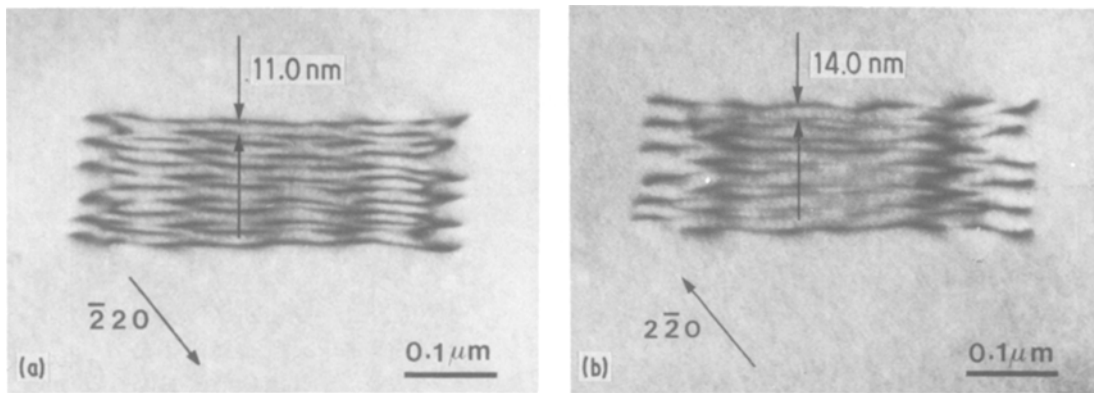


Figure 5 An example of the change in dislocation image spacing observed with equal and opposite diffracting g -vectors. (Alloy 800, $\epsilon = 5\%$). (a) $g = 2\bar{2}0$; (b) $g = \bar{2}20$.

posite sign by observing the change in spacing between dislocation images obtained with equal and opposite diffracting vectors [7]. An example of this is shown in Fig. 5a and b, where the apparent spacing between dislocations changes from 11.0 nm (operating reflection $\bar{2}22$) to 14.0 nm (operating reflection $2\bar{2}0$). Similarly, when the multipoles were steeply inclined to the foil surface, the opposite sign of adjacent Burgers vectors could be deduced by using the centre of inversion symmetry [8] (for example see Fig. 6a).

In cases where the individual dislocations were closely spaced it was often found that they could not be resolved using standard two-beam diffracting conditions, (Fig. 6a). However, under weak-beam imaging conditions, the constituent dislocations were clearly resolved. In this manner, it is shown that the multipole shown in Fig. 6a consists of six dipoles (see Fig. 6b).

Many of the multipoles observed in this work

were somewhat irregular in character. For example, it was sometimes found that individual dislocations change dipolar partners within a multipole (see Fig. 4). Trace analysis of a number of multipoles in specimens which had undergone secondary creep showed that, in general, they did not lie exactly on $\{111\}$ planes (see also Section 3.3). Other multipoles were very loosely associated. Fig. 7 shows an array of dislocations in the process of forming a multipole in material crept to a strain of 1% at $\sigma = 30$ MPa. In this instance the multipole and the more loosely-bound dislocations form a planar array.

3.3. Observation of multipoles in AISI 316 L

An example of a multipole observed in AISI 316L crept for 22 h at $\sigma = 150$ MPa is shown in Fig. 8. Although the general characteristics of the multipoles observed in this alloy were similar to those

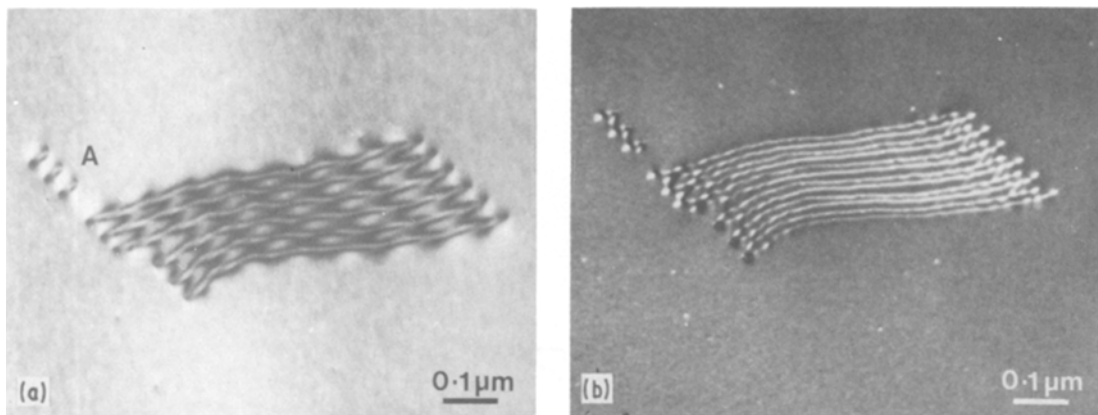


Figure 6 An illustration of the use of the weak-beam technique to resolve closely-spaced dislocations (Alloy 800, $\epsilon = 5\%$). A multipole which is steeply inclined to the foil surface. Note both the centre of inversion symmetry at the multipole and the dislocation loops at A. (b) A weak-beam image of the same multipole.

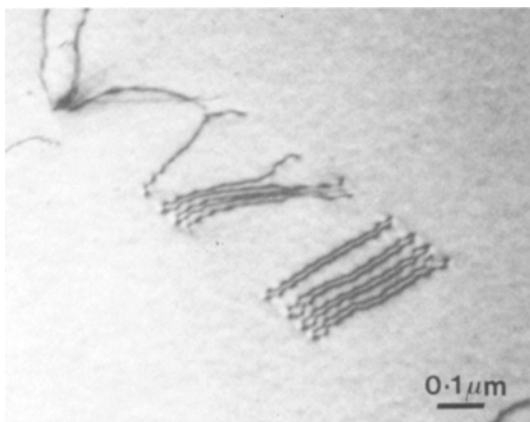


Figure 7 An ill-formed multipole in Alloy 800 deformed to $\epsilon = 1\%$. The dislocations in this configuration lie on $\{111\}$ planes.

described for Alloy 800, certain important differences were observed. For example, the multipoles tended to be more regular in appearance and often contained a much larger number of dislocations. Also, in contrast to Alloy 800, trace analysis showed that multipoles in AISI 316L were confined to $\{111\}$ planes. A striking example illustrating these two points is shown in Fig. 9a. This highly planar multipole consists of 38 separate dipoles. The fact that it lies on a $\{111\}$ plane may be gauged by comparing the intersections of the multipole with the foil surfaces with those at the twin interface situated at A (see Fig. 9a). It is also interesting to note that there is a gradual variation in the directions of the lines of the individual dislocations indicating that the dislocations cannot be purely edge in character.

The multipole shown in Fig. 9a was found to

be unstable when the thin foil was left in vacuum. Fig. 9b shows the same area after the specimen had been left in the microscope overnight without the electron beam turned on. During this period, the multipole decomposed to leave behind some dislocation loops (D in Fig. 9b), helical dislocations and a few loosely-arranged dipoles. It can be noted that similar small dislocation loops can be seen adjacent to one of the multipoles seen in Alloy 800 and shown in Fig. 6.

4. Discussion

The previous sections have shown that multipoles can be observed in two austenitic stainless steels after they have undergone high-temperature power-law creep. The arrays of dislocations are similar to the multipoles which have been found in certain fcc alloys after low-strain ambient-temperature deformation [9]. Indeed, planar multipoles lying on $\{111\}$ planes have been reported for an 18 wt% Cr, 10 wt% Ni, austenitic stainless steel after 1 to 3% tensile strain at room temperature [10].

The planar $\{111\}$ nature of the multipoles observed in AISI 316L and in the primary creep stage in Alloy 800 implies that they were formed by the interaction of glide dislocations on adjacent parallel slip planes. Most probably, this occurs either during the "instantaneous" deformation on application of the load or during the very early stages of creep. The requirement of planar slip could also explain why multipoles were not observed at stresses below a critical value (30 MPa for Alloy 800 at 800°C, 150 MPa for AISI 316L at 650°C). Supportive evidence for the multipoles

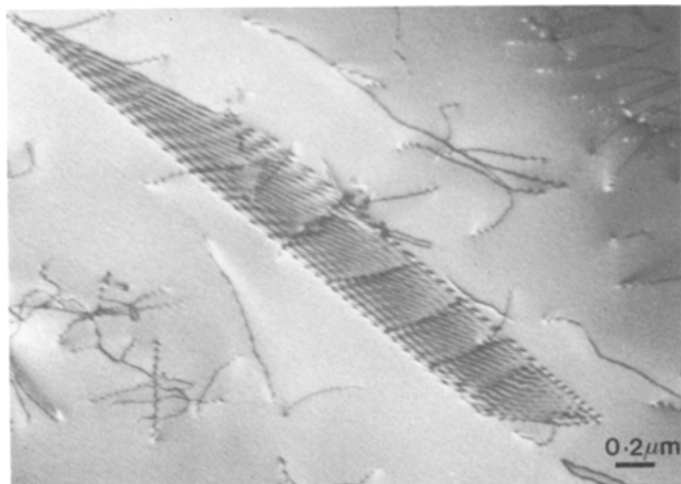


Figure 8 A multipole in AISI 316L consisting of approximately 60 dislocations. The dislocations in this multipole lie on a $\{111\}$ plane.

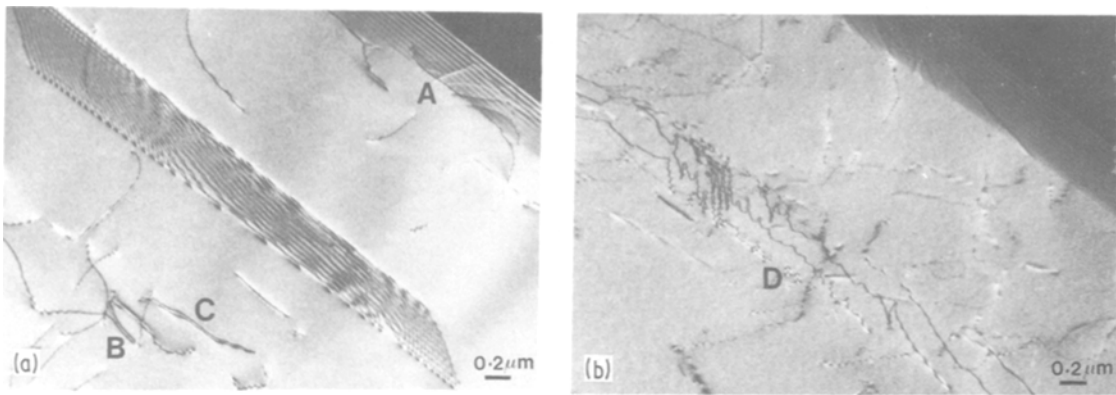


Figure 9 (a) An example of a very large multipole in AISI 316L consisting of 38 separate dipoles. By comparing the traces of this multipole to that of the coherent twin at A it can be seen that the multipole lies on a $\{111\}$ plane. Note also the dipoles at B and C. (b) The same area as that shown in (a) after being left in vacuum overnight. The multipole has decomposed to produce some dislocation loops (D), helical dislocations and some dipoles.

being created at the early stages of the creep test comes from the fact that no noticeable increase in the density of multipoles was found with increasing strain (from 1 to 10%) in Alloy 800.

Both the lack of dislocation pinning in the fully-aged Alloy 800 and the higher creep temperature employed for this material offer a ready explanation for the poorer regularity of the multipoles in Alloy 800 compared with those found in AISI 316L and also for the fact that they were not always situated on $\{111\}$ planes during secondary creep: if not pinned, a multipole can either climb as a unit or individual dipoles in the multipole can climb by the diffusion of vacancies over very short distances between dislocations of opposite sign.

Loops of the type shown in Fig. 6 can be formed by a simple pinching-off of dipoles. In this context the instability, in a thin foil, of the multipole shown in Fig. 9 is of interest. One possible explanation for this is that the dislocations in the multipole were pinned by interstitial Cottrell atmospheres as well as by strain field interactions. The interstitials could readily escape to the foil surface via pipe-diffusion along the dislocations. This in itself need not necessarily render a multipole unstable since many other multipoles remained stable in thin foils stored in vacuum for times as long as two years. However, the particular multipole of Fig. 9 obviously contained dislocations with a significant screw component. Once unpinning had occurred these dislocations could easily cross-slip to the foil surface.

Finally, it is interesting to note that in 1957 Weertman [11] predicted the formation of multipoles during creep and he used multipole forma-

tion as the basis for a dislocation climb creep model. The present observations indicate that, although multipoles may not be of major significance for steady-state creep, as was originally suggested, they may well be a common feature of the early stages of creep strain in alloys deformed under relatively high stress conditions.

5. Conclusions

(a) Multipoles have been observed after power-law creep of two austenitic stainless steels.

(b) The multipoles consist of a series of dipoles held together by the interaction between dislocation strain fields of opposite sign.

(c) The number of multipoles remains approximately constant with increasing strain from primary to secondary creep.

(d) Multipoles in AISI 316L were always found to lie on $\{111\}$ planes. This was not necessarily the case in Alloy 800.

(e) The accumulated evidence suggests that multipoles form by the interaction of glide dislocations on adjacent parallel slip planes either during "instantaneous" deformation on application of the load or during the very early stages of primary creep.

Acknowledgements

Financial support was received from the Science Research Council (UK), the Swedish Board for Technical Development, the Swedish Natural Science Research Council and the Danish Council for Scientific and Industrial Research. The authors are also grateful to Sandvik AB and Uddeholm AB for the supply of materials.

References

1. J. GITTUS, "Creep, Viscoelasticity and Creep Fracture in Solids" (Applied Science Publishers, London, 1975).
2. H. M. MIEKK-OJA and V. K. LINDROOS. *Surface Sci.* **31** (1972) 422.
3. A. ORLOVA, M. PAHUTOVA and J. CADEK, *Phil. Mag.* **25** (1971) 865.
4. H. MODEER and R. LAGNEBORG, *Jernkont. Ann.* **155** (1971) 363.
5. J. O. NILSSON, P. R. HOWELL and G. L. DUNLOP. *Acta Met.* **27** (1979) 179.
6. A. HORSEWELL, *Met. Trans. A* **9** (1978) 1843.
7. W. BELL, W. Z. ROSER and G. THOMAS. *Acta Met.* **12** (1964) 1247.
8. C. FORWOOD and P. HUMBLE. *Australian J. Phys.* **23** (1970) 697.
9. E. WINTER and H. P. KARNTHALER, *Acta Met.* **26** (1978) 941.
10. J. S. T. VAN ASWEGEN, R. W. K. HONEYCOMBE and D. H. WARRINGTON, *Acta Met.* **12** (1964) 1.
11. J. WEERTMAN. *J. App. Phys.* **28** (1957) 362.

Received 27 February and accepted 26 March 1981.